

Thermodynamic studies of the two dimensional Falicov-Kimball model on a triangular lattice

Umesh K. Yadav, T. Maitra, and Ishwar Singh

Department of Physics, Indian Institute of Technology Roorkee, Roorkee- 247667, Uttarakhand, India

the date of receipt and acceptance should be inserted later

Abstract. Thermodynamic properties of the spinless Falicov-Kimball model are studied on a triangular lattice using numerical diagonalization technique with Monte-Carlo simulation algorithm. Discontinuous metal-insulator transition is observed at finite temperature. Unlike the case of square lattice, here we observe that the finite temperature effect is not able to smear out the discontinuous metal-insulator transition seen in the ground state. Calculation of specific heat (C_v) shows single and double peak structures for different values of parameters like on-site correlation strength (U), f -electron energy (E_f) and temperature.

PACS. 71.45.Lr Charge-density-wave systems – 71.30.+h Metal-insulator transitions and other electronic transitions – 64.75.Gh Phase separation and segregation in model systems

1 Introduction

The Falicov-Kimball model (FKM) [1] is one of the simplest and most successful model for the correlated electron systems. This model was introduced to describe the semiconductor-metal transition in mixed-valence compounds and rare-earth systems. Recently systems such as transition-metal dichalcogenides [2, 3, 4], cobaltates [5], GdI_2 [6, 7] and its doped variant GdI_2H_x [8] have attracted considerable attention as they exhibit remarkable cooperative phenomena, like metal-insulator transition, charge and magnetic order, excitonic instability [2] and possible non-Fermi liquid states [7, 9]. These systems are characterized by the presence of localized and itinerant electrons confined to the two-dimensional triangular lattice.

In the FKM effective interactions are mediated by band electrons [10, 11]. Therefore, the model has also been studied as a model of crystallization, for example, as a model of binary alloy. The model describes the systems exhibiting different types of phase configurations e.g. regular phase [12], phase separation [13, 14, 15, 16, 17] and stripe phases [18, 19, 20]. There are predominantly more rigorous results available for the FKM on a bipartite lattice than on non-bipartite lattices. On a bipartite lattice, one of the most important result proved by Kennedy and Lieb [10, 11] is that at low enough temperature the half-filled FKM possesses a long range order, i.e., the localized electrons form a checkerboard pattern, the same as in the ground state. This result holds for arbitrary bipartite lattices in dimensions $d \geq 2$ and for all values of on-site Coulomb correlation strength U .

Recently few interesting results are reported for the phase diagram of localized f -electrons due to the inclusion of correlated hopping (t') [21, 22, 23, 24, 25, 26, 27] of

itinerant electrons in FKM. Phase segregation, even in weak correlation limit ($U \sim 0.5$ or 1), is one of the most striking outcome of the generalization of the FKM on bipartite [14, 26, 28] and on non-bipartite [27] lattices.

Even though the FKM is one of the simplest models for correlated electrons, a clear picture of metal-insulator transition in FKM is still debated for many years. Metal-insulator transition strongly depends upon the choice of the d -electron density of states (DOS). There are only few exact results available on metal-insulator transition on a non-bipartite lattice [27, 29, 30]. In a recent work [27] we have studied the ground state properties of the Falicov-Kimball Model on a triangular lattice with correlated hopping and observed first order phase transition in the $f(d)$ -electron occupation at particular value of f -electron energy E_f . This shows that the small change in the lattice parameter by means of introducing impurity or by applying pressure one can successfully explain the valence and metal-insulator transitions. In a separate work [30] we studied the effects of Coulomb repulsion between f - and d -electrons (U) and also between f -electrons (U_f) themselves in a two-fold degenerate f -level on the ground state properties. We observed first order (discontinuous) insulator-metal transition at particular values of U and U_f .

A very important question, in this context arises as to what is the nature of these phase-transitions at finite temperature? Does this model again give the first order (discontinuous) insulator to metal transitions of $f(d)$ -electron occupation with E_f and temperature? In addition it is also interesting to know the dependence of the specific heat (C_v) on temperature for different range of parameter values.

In this work, therefore, we study the FKM in its spinless version numerically for all ranges of interactions, and

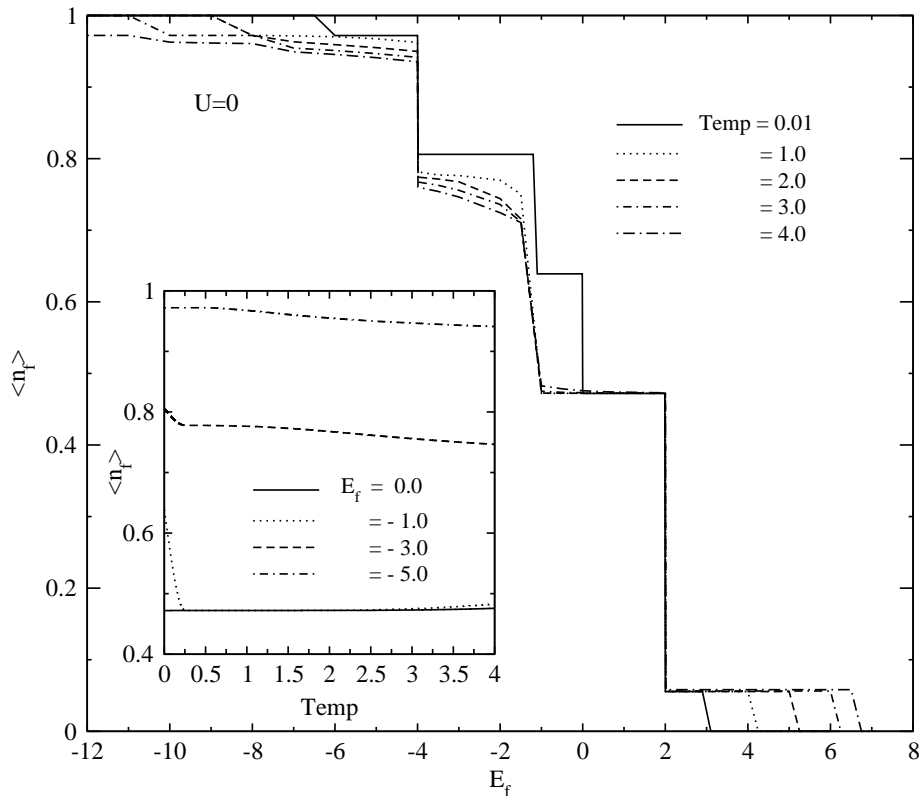


Fig. 1. $(n_f - E_f)$ phase diagram for different values of temperature at $U=0$ and temperature dependence of the f -electron occupation number n_f at $U = 0$ for different values of E_f (shown in inset).

explore the metal-insulator transition and specific heat on a triangular lattice at finite temperature.

The Hamiltonian of the system may be written as

$$H = - \sum_{\langle ij \rangle} (t_{ij} + \mu \delta_{ij}) d_i^\dagger d_j + E_f \sum_i f_i^\dagger f_i + U \sum_i f_i^\dagger f_i d_i^\dagger d_i. \quad (1)$$

Here d_i^\dagger, d_i (f_i^\dagger, f_i) are, respectively, the creation and annihilation operators for itinerant d -electrons (localized f -electrons) at the site i . The first term in Eq.(1) is a measure of kinetic energy of d -electrons on a triangular lattice: only nearest-neighbor hopping is considered. The second term represents the dispersionless energy level E_f of the f -electrons while the third term is the on-site Coulomb repulsion between d - and f -electrons.

2 Methodology

In the Hamiltonian (1), hybridization between d - and f -electrons is absent. Therefore, local f -electron occupation number $\hat{n}_{f,i} = f_i^\dagger f_i$, is conserved. The $\omega_i = f_i^\dagger f_i$ is a good quantum number as $[\hat{n}_{f,i}, H] = 0$ taking values either 1 or 0, according to the whether site i is occupied or unoccupied by an f -electron. Due to the local conservation

of f -electron number the Hamiltonian (1) may be written as,

$$H = \sum_{\langle ij \rangle} h_{ij}(\omega) d_i^\dagger d_j + E_f \sum_i \omega_i \quad (2)$$

where $h_{ij}(\omega) = -t_{ij} + (U\omega_i - \mu)\delta_{ij}$.

We set the hopping integral $t_{ij} = 1$, for nearest neighboring sites i and j and $t_{ij} = 0$, otherwise. The eigenvalue spectrum of the Hamiltonian H , for a configuration ω of f -electrons is calculated by numerical diagonalization on a triangular lattice of finite size with periodic boundary conditions (PBC). The average value of physical quantities is obtained by the classical Monte Carlo method using Metropolis algorithm. The details of the method can be found in our earlier papers [27,30].

We work at half-filling, i.e., $N_f + N_d = N$ where N_f, N_d are the total number of f - and d -electrons and $N = L^2$ ($L = 6$) is the total number of sites. At a finite temperature T , the thermodynamic quantities are determined as averages over various configurations $\omega(N_f)$ with statistical weight $P(\omega(N_f))$ given by

$$P(\omega(N_f)) = \frac{e^{-\beta F(\omega(N_f))}}{\mathcal{Z}} \quad (3)$$

where the corresponding free energy is given as,

$$F(\omega) = -\frac{1}{\beta} \left[\ln \left(\prod_i e^{-\beta E_f \omega_i} \right) \right]$$

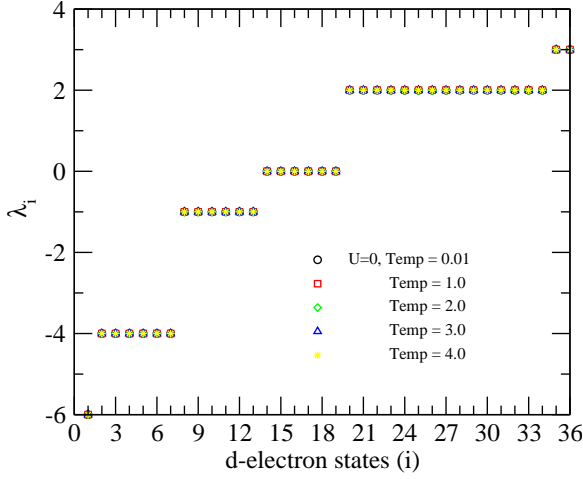


Fig. 2. (color online) The d-electron energy spectrum for $U=0$.

$$+ \sum_j \ln(e^{-[\lambda_j(\omega(N_f)) - \mu]\beta} + 1), \quad (4)$$

with μ being the chemical potential. The μ has been fixed to satisfy the condition $n_f + n_d = 1$.

The partition function is

$$\mathcal{Z} = \prod_i \left(\sum_{\omega_i=0,1} e^{-\beta E_f \omega_i} \right) \prod_j \left(1 + e^{-\beta[\lambda_j(\omega(N_f)) - \mu]} \right). \quad (5)$$

Let a thermodynamic quantity ‘A’ have value $A(\omega(N_f))$ corresponding to the configuration $\omega(N_f)$ of N_f -electrons, then the ensemble average of ‘A’ at temperature T is obtained as

$$\langle A \rangle = \frac{\sum_{N_f} \sum_{\omega} A(\omega(N_f)) e^{-\beta F(\omega(N_f))}}{\mathcal{Z}} \quad (6)$$

For example the ensemble average of number of f-electrons for given values of U , E_f , T is obtained as

$$\langle N_f \rangle = \frac{\sum_{N_f} \sum_{\omega} N_f(\omega(N_f)) e^{-\beta F(\omega(N_f))}}{\mathcal{Z}} \quad (7)$$

and $n_f = \langle n_f \rangle = \frac{\langle N_f \rangle}{N}$.

The total internal energy $E(\omega)$ of the system corresponding to the configuration $\omega(N_f)$ is given as,

$$E(\omega(N_f)) = \sum_i \frac{\lambda_i(\omega)}{e^{(\lambda_i(\omega) - \mu)\beta} + 1} + E_f N_f(\omega) \quad (8)$$

The specific heat (C_v) is calculated from the fluctuation-dissipation theorem (FDT). The specific heat is related through the FDT to the internal energy and defined as,

$$C_v = \frac{1}{N} \frac{1}{kT^2} (\langle E^2 \rangle - \langle E \rangle^2), \quad (9)$$

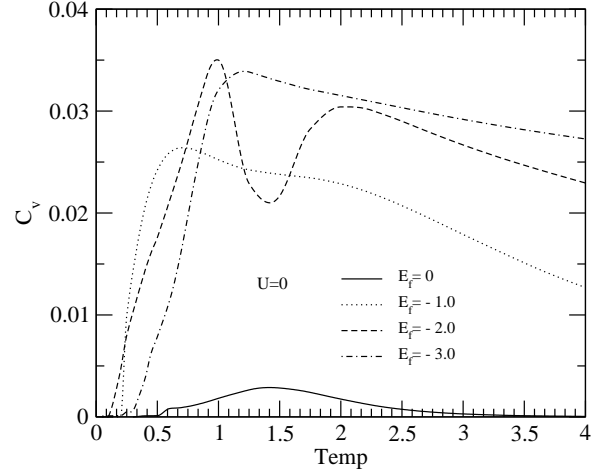


Fig. 3. Specific heat (C_v) as a function of temperature calculated at $U = 0$ for different values of E_f .

3 Results and discussion

3.1 Noninteracting case ($U=0$)

We firstly study the noninteracting case ($U = 0$). Using the method described above, we have found average value of f-electron occupation number per site $n_f = \langle n_f \rangle = \frac{\langle N_f \rangle}{N}$ as a function of E_f at different temperatures. Also we have calculated specific heat C_v as a function of temperature for different values of E_f . In Fig.1 we have shown n_f as a function of E_f for different temperatures and also as a function of temperature for different values of E_f (shown in inset of Fig.1). In Fig.2 we show the d-electron energy spectrum corresponding to the configuration $\omega(N_f)$ with minimum internal energy.

When E_f is changed upwards (starting from the bottom of conduction band), n_f is found to decrease suddenly at some particular positions of E_f . For example at $E_f = -4.0$, n_f decreases abruptly from $n_f \sim 0.98$ to $n_f = 0.8$, at $E_f = -1.0$, from 0.8 to 0.6 at $E_f = 0.0$, from 0.6 to ~ 0.48 and at $E_f = 2.0$, from 0.48 to ~ 0.03 . If we look at the d-electron energy spectrum, we find d-levels at energy $E = -4.0, -1.0, 0.0, 2.0$; i.e. there are energy gaps [31] in d-electron spectrum in energy range $[-4, -1]$, $[-1, 0]$, $[0, 2]$. As $n_f + n_d = 1$, the chemical potential μ is pinned at E_f . So, as E_f is shifted upward, μ shifts upward. When μ shifts from -4 to -1, there being no d-levels in this range, n_d remains constant and so should n_f . This is exactly what we find as shown in Fig.1. As μ reaches the energy -1, where there are many d-levels available, these get occupied and n_f decreases abruptly. Now with the increase of temperature, d-states above chemical potential are also occupied fractionally. That is why n_f decreases a bit as temperature increases. However, in contrast to the case of bipartite lattice [32], temperature is unable to smear out the discontinuous transition on the triangular lattice. Variation of n_f with temperature at different E_f is shown in the inset of Fig.1. When E_f is near the bottom of the d-band, n_f is near unity at $T \rightarrow 0$ and decreases slowly as T is

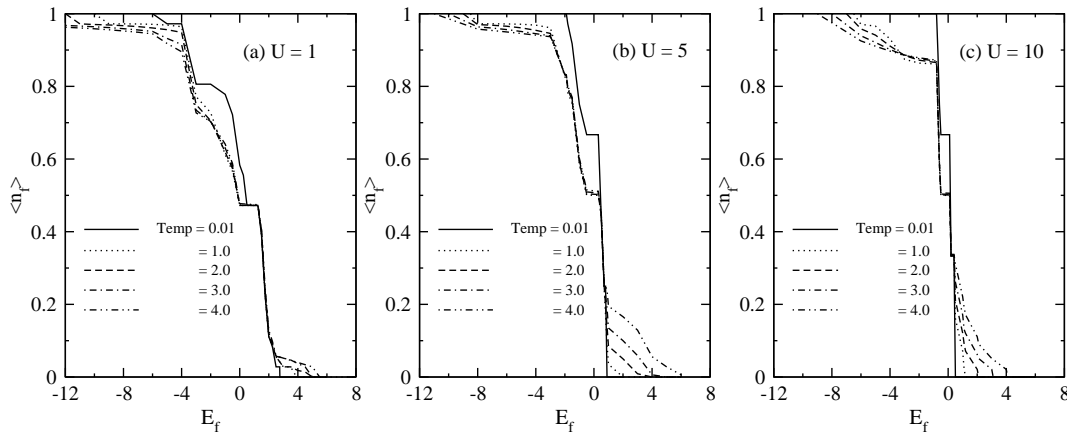


Fig. 4. $(n_f - E_f)$ phase diagram for different values of temperature calculated at (a) $U = 1$, (b) $U = 5$ and (c) $U = 10$.

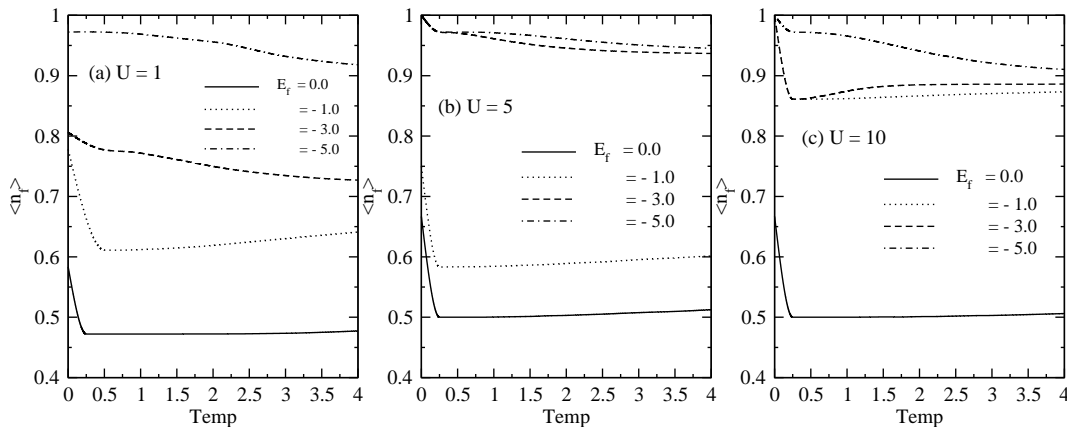


Fig. 5. Temperature dependence of the f-electron occupation number n_f at (a) $U = 1$, (b) $U = 5$ and (c) $U = 10$ for different values of E_f .

increased. At other positions of E_f , n_f is lesser than unity (and the system is in classical mixed-valent regime) and decreases slowly as T is increased.

Shown in Fig.3 is the specific heat C_v as a function of temperature for different positions of E_f . A broad single peak is observed in specific heat curve at all values of E_f except at $E_f = -2.0$. At $E_f = -2.0$ there are two peaks (one sharp peak followed by a broad peak). At low temperature we observe that variation in C_v deviates from the linear behavior of free electrons. The nature of the peaks in the specific heat curves could be understood if we compare these with the d-electron energy spectrum (shown in Fig.2) for different temperatures. The d-electron spectrum does not depend on N_f , E_f and temperatures. The spectrum is discrete and multi-gaped. Wide gap around Fermi energy in d-electron spectrum corresponds to broad peak and small gap corresponds to sharp peak in C_v .

3.2 Finite interaction case ($U \neq 0$)

Let us consider the case where Coulomb correlation U between d-and f- electrons is finite. Fig.4(a), (b) and (c)

show $(n_f - E_f)$ phase diagrams for $U=1, 5$ and 10 and for temperatures $0.01, 1, 2, 3$ and 4 respectively. We observe that for $U=1$, as temperature increases from 0.01 to 4 , the valence transition (i.e. n_f -transition) (i) occurs at higher values of E_f and (ii) becomes smoother. We observe that the transition width (the range of E_f over which n_f goes from 1 to 0), increases as temperature increases from 0.01 to 4 .

At $U=5$ and 10 the $(n_f - E_f)$ -transition at different temperatures shows behavior similar to $U=1$ for E_f well below or well above the middle of the conduction band. When E_f is near the middle of the conduction band, further increment in the temperature does not affect the n_f -transition significantly. This phenomena could be explained by the large gap in the many body states around the Fermi energy (E_F). Due to large gap at the Fermi energy (see Fig.7 (b) and (c) for $U=5$ and 10 respectively) even higher temperature is not sufficient to move the localized f-electrons to the higher d-states.

Fig.5(a), (b) and (c) show variation of n_f with temperature for $U=1, 5$ and 10 and for different E_f positions. We observe that for all values of U , n_f approaches towards the value around 0.5 at high temperatures. At low tem-

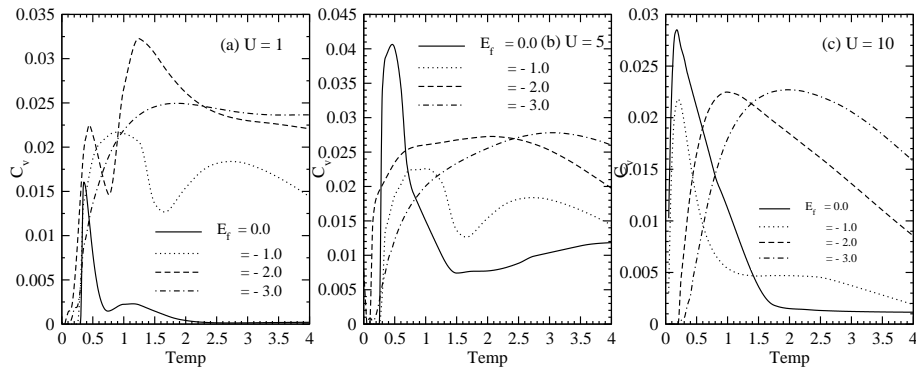


Fig. 6. Specific heat (C_v) as a function of temperature calculated at (a) $U = 1$, (b) $U = 5$ and (c) $U = 10$ for different values of E_f .

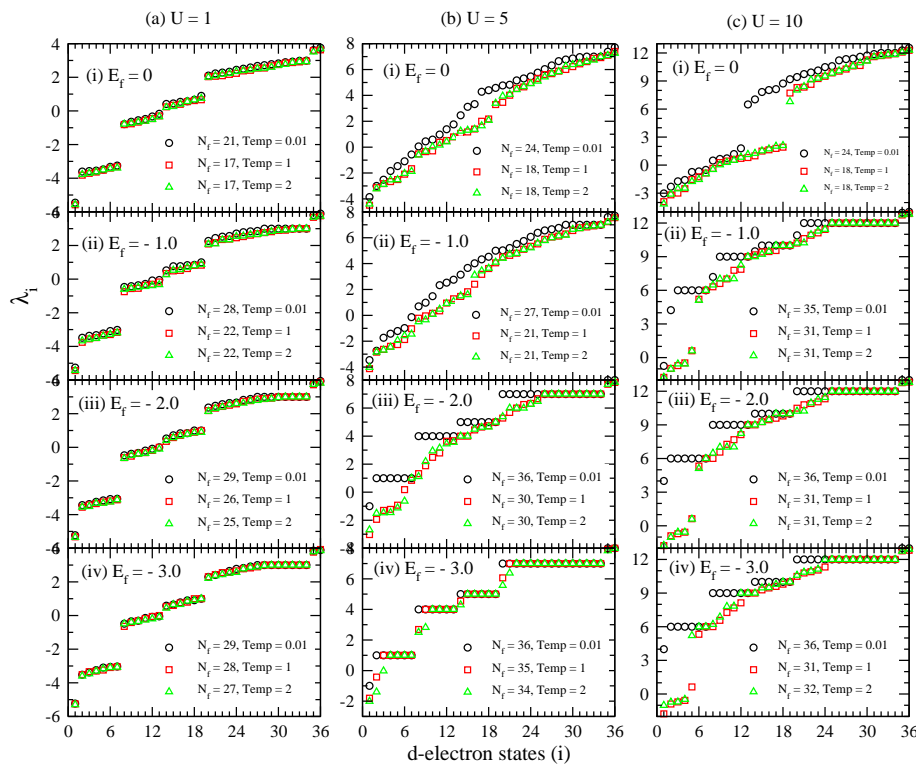


Fig. 7. (color online) The d-electron energy spectrum for different values of temperature and E_f calculated at (a) $U=1$, (b) $U=5$ and (c) $U=10$.

peratures n_f takes values in the range $[0.5, 1.0]$ depending upon the values of U and E_f . Our results are in contrast to the results of P. Farkasovsky [32] obtained on bipartite lattice. We observed discontinuous $(n_f - E_f)$ transitions with temperature. We report that even higher temperature is not sufficient to smear the discontinuous $(n_f - E_f)$ transition observed in ground state spinless FKM on triangular lattice [27,30]. They observed smooth variation in n_f as a function of temperature. The contrast between these two results are due to the choice of different lattices. In square (bipartite) lattice, energy spectrum of the d- electrons are symmetric about the middle of the conduction band, while in triangular (non-bipartite) lattice

the d-electron energy spectrum is asymmetric about the middle of the conduction band and large number of d-electron states lie in the small regime above the middle of the conduction band.

In Fig.6(a), (b) and (c) we have shown variation of C_v with temperature for $U=1, 5$ and 10 at different E_f positions. In the small Coulomb correlation limit (say $U=1$) and E_f at the bottom of the conduction band ($E_f = -3.0$), a single broad peak in C_v is observed. Moving the f-electron energy level towards the middle of conduction band two peak pattern (one sharp followed by a broad peak) is observed. For E_f at center of conduction band a sharp peak followed by a low broad peak is observed.

These different peaks can be explained by the energy spectrum of the d-electrons shown in Fig.7(a). In this figure we have shown the d-electron energy spectrum corresponding to the configuration $\omega(N_f)$ with minimum internal energy. The d-electron spectrum is multi-gaped and depends upon the temperature and E_f . For $U=1$, $E_f=0$ and for low temperature, a gapless spectrum is observed. At finite temperature, we observe a gap around chemical potential in d-electron spectrum. Moving E_f from middle to bottom of conduction band say $E_f = -2$, a large gap is observed at low temperature. The gap disappears at higher temperatures. The small gap in d-electron spectrum leads to a sharp peak while large gap corresponds to a broad peak in C_v .

For $U=5$ and E_f at the bottom of conduction band a broad peak in C_v is observed. Width of peak is reduced by moving f-electron level towards middle of conduction band. Two broad peaks in C_v at $E_f = -1.0$ are observed. A single peak is observed at $E_f=0$. At $U=10$, a single peak is observed in C_v for all observed E_f values. The width of the peak in C_v decreases with moving E_f from bottom to middle of conduction band. The critical temperature (T_c) at which peak occurs in C_v , reduces as E_f moves from bottom to middle of conduction band. If we compare T_c for $E_f=0$ and at different U -values we observe that T_c goes on decreasing with increasing U , similar to the result observed by M. Maska [29]. These features are well explained on the basis of variation of d-electron spectrum with E_f and temperature shown in Fig.7(b) and (c) for $U=5$ and 10 respectively.

In conclusion, we have studied the spinless Falicov-Kimball model on a triangular lattice at finite temperature. The nature of metal-insulator transition with temperature has been looked into in various parameter regime. The temperature dependence of specific heat (C_v) is also studied for different ranges of parameters like U , E_f . Discontinuous metal-insulator transition is observed even at finite temperature. This is unlike the case of bipartite lattices where it has been reported that with temperature metal-insulator transition becomes second order in nature. But here we see that the temperature can not smear the discontinuous metal-insulator transition observed in ground state on triangular lattice. Single and double peak patterns are observed in C_v depending on the parameters U , E_f and temperature. It is proposed that the various features could be explained by many body spectrum of d -electrons.

Acknowledgments. UKY acknowledges CSIR, India for research fellowship.

References

1. L. M. Falicov and J. C. Kimball, Phys. Rev. Lett. **22**, 997 (1969).
2. H. Cercellier, C. Monney, F. Clerc, C. Battaglia, L. Despont, M. G. Garnier, H. Beck, and P. Aebi, Phys. Rev. Lett. **99**, 146403 (2007).
3. E. Morosan, H. W. Zandbergen, B. S. Dennis, J. W. G. Bos, Y. Onose, T. Klimczuk, A. P. Ramirez, N. P. Ong, and R. J. Cava, Nature Phys. **2**, 544 (2006); D. Qian, D. Hsieh, L. Wray, E. Morosan, N. L. Wang, Y. Xia, R. J. Cava, and M.Z. Hasan, Phys. Rev. Lett. **98**, 117007 (2007); G. Li, W. Z. Hu, D. Qian, D. Hsieh, M. Z. Hasan, E. Morosan, R. J. Cava, and N. L. Wang, Phys. Rev. Lett. **99**, 027404 (2007).
4. K. E. Wagner, E. Morosan, Y. S. Hor, J. Tao, Y. Zhu, T. Sanders, T. M. McQueen, H. W. Zandbergen, A. J. Williams, D. V. West, and R. J. Cava, Phys. Rev. B **78**, 104520 (2008).
5. D. Qian, D. Hsieh, L. Wray, Y. D. Chuang, A. Fedorov, D. Wu, J. L. Luo, N. L. Wang, L. Viciu, R. J. Cava, and M. Z. Hasan, Phys. Rev. Lett. **96**, 216405 (2006).
6. C. Felser, K. Ahn, R. K. Kremer, R. Seshadri, and A. Simon, Solid State Chem., **147**, 19 (1999).
7. A. Taraphder, L. Craco and M. Laad, Phys. Rev. Lett. **101**, 136410 (2008).
8. T. Maitra, A. Taraphder, A. N. Yaresko, and P. Fulde, Euro. Phys. Journal B **49**, 433 (2006).
9. A. H. Castro Neto, Phys. Rev. Lett. **86**, 4383 (2001).
10. T. Kennedy, Rev. Math. Phys. **6**, 901 (1994); T. Kennedy and E. H. Lieb, Physica A **138**, 320 (1986).
11. E. H. Lieb, Physica A **140**, 240 (1986).
12. M. Maska and K. Czajka, Phys. Rev. B **74**, 035109 (2006).
13. J. K. Freericks, R. Lemanski, Phys. Rev. B **61**, 13438, (2000).
14. J. K. Freericks, E. H. Lieb and D. Ueltschi, Phys. Rev. Lett. **88**, 106401 (2002); Comm. Math. Phys. **227**, 243 (2002).
15. B. M. Letfulov and J. K. Freericks, Phys. Rev. B **66**, 033102, (2002).
16. J. K. Freericks, Ch. Gruber and N. Macris, Phys. Rev. B **60**, 1617 (1999); **53**, 16189 (1996).
17. P. Farkasovsky, Phys. Rev. B **60**, 10776 (2000).
18. R. Lemanski, J. K. Freericks and G. Banach, Phys. Rev. Lett. **89**, 196403, (2002).
19. R. Lemanski, J. K. Freericks and G. Banach, J. Stat. Phys. **116**, 699, (2004).
20. K. Haller and T. Kennedy, J. Stat. Phys. **102**, 15, (2001).
21. J. Wojtkiewicz and R. Lemanski, Phys. Rev. B **64**, 233103 (2001).
22. J. E. Hirsch, Phys. Rev. B **39**, 11515 (1989).
23. B. R. Bulka, Phys. Rev. B **57**, 10303 (1998).
24. A. Shvaika, Phys. Rev. B **67**, 075101 (2003).
25. P. Farkasovsky and N. Hudakova, J. Phys. Cond-mat. **14**, 499 (2002).
26. H. Cenkarikova and P. Farkasovsky, Phys. Stat. Sol.(b) **242**, 2061 (2005).
27. Umesh K Yadav, T. Maitra, Ishwar Singh and A. Taraphder, J. Phys.: Condens. Matter **22**, 295602 (2010); Umesh K Yadav, Tulika Maitra and Ishwar Singh, Proc., DAE-SSPS, **54**, 1065 (2009).
28. T. Kennedy, J. Stat. Phys. **91**, 829 (1998); **102**, 15 (2001).
29. K. Czajka and M. Maska, Physica B **378-380**, 275-277 (2006).
30. Umesh K Yadav, T. Maitra, Ishwar Singh, and A. Taraphder, EPL, **93**, 47013 (2011).
31. The definition of the gap [10] used here $\Delta = E(N_d + 1, N_f) + E(N_d - 1, N_f) - 2E(N_d, N_f)$ necessarily requires relaxing the condition $n_d + n_f = 1$ to order $\frac{1}{N}$.
32. P. Farkasovsky, Z. Phys. B **102**, 91 (1997); P. Farkasovsky, Phys. Rev. B **54**, 7865 (1996).